scientific reports

Check for updates

OPEN

Hepatoprotective effect of *Thymus vulgaris* extract on sodium nitrite-induced changes in oxidative stress, antioxidant and inflammatory marker expression

Mohamed Mohamed Soliman[1,2]✉, Adil Aldhahrani[1] & Mohammed M. M. Metwally[3]

The herb thyme (*Thymus vulgaris*) has multiple therapeutic uses. In this study, we explored how *T. vulgaris* leaf extract protects liver cells against sodium nitrite-($NaNO_2$) induced oxidative stress. Mice were divided into four groups; each group received one of the following treatments orally: saline; *T. vulgaris* extract alone; $NaNO_2$ alone; *or T. vulgaris* extract + $NaNO_2$. Alanine aminotransferase (ALT), aspartate aminotransferase (AST), reduced glutathione (GSH), superoxide dismutase (SOD), malondialdehyde (MDA), IL-1β, IL-6, TNF-α, and total proteins were measured in serum using standard methods. TNF-α, hemooxygenase-1 (HO-1), thioredoxin, SOD, and GSH synthase, all of which are linked to oxidative stress, were measured using quantitative real-time PCR (qRT-PCR). In mice treated with *T. vulgaris* extract, the effect of $NaNO_2$ on ALT and AST levels and total proteins was reduced, and its effect on antioxidant levels was reversed. Normally, $NaNO_2$ causes hepatocyte congestion and severe hepatic central vein congestion. Tissues in the mice treated with *T. vulgaris* were restored to normal conditions. Our results demonstrate that $NaNO_2$-induced hepatic injury is significantly reduced by pretreatment with *T. vulgaris* extract, which protects against hepatic oxidative stress and its associated genes at the biochemical, molecular, and cellular levels.

Nitrite is important to organ health. At very low concentrations, and within physiological levels, nitrite has antioxidant properties[1,2]. When reduced to nitric oxide (NO), which is critical for vascular homeostasis[3], it plays a critical role in cell signaling, cellular immunity, and in the activation of certain regulatory proteins[3,4]. These regulatory proteins are vital to the maintenance of normal human health.

Human beings use nitrites in a wide variety of ways, which makes them hard to avoid. In industry, nitrite and its salts are used in preservatives, colorants, and in manufacturing rubber products and dyes; in food, nitrite is employed for its anti-microbial properties; and in medicine, it is used to treat cyanide poisoning, ischemic heart disease, and as a vasodilator[5–7]. Environmentally, improper waste disposal, over-reliance on nitrite-based fertilizers, and excessive use in food preservatives has led to chronic exposure and the accumulation of high nitrite-nitrate levels in humans.

Overexposure (due either to high concentrations or prolonged low-dose exposure) is toxic and can cause liver, kidney, or other organ failure[8], methemoglobinemia[9], and eventually death. Overexposure in humans occurs primarily through contaminated food or drinking water. After first affecting the GI tract, it passes into the circulation, where it reaches various other organs[10], causing further oxidative stress and toxicity. It has been observed that oxidative stress is a key mediator of nitrite-induced oxidative damage[11] and that treatment with antioxidants can ameliorate or even reverse this[12]. The possible mechanism by which $NaNO_2$ decreases antioxidant enzyme

[1]Clinical Laboratory Sciences Department, Turabah University College, Taif University, P.O. Box 11099, Taif 21944, Saudi Arabia. [2]Biochemistry Department, Faculty of Veterinary Medicine, Benha University, Benha 13736, Egypt. [3]Department of Pathology, Faculty of Veterinary Medicine, Zagazig University, Zagazig 44519, Egypt. ✉email: mmsoliman@tu.edu.sa

activity is induction of reactive oxygen species (ROS), which mediate the oxidation of enzyme molecules or the binding of NO[13].

In the liver, $NaNO_2$ induced hepatic toxicity through inhibition of antioxidant activity and increasing the levels of pro-inflammatory cytokines[14]. Liver disease is often treated using synthetic chemical drugs, but these can cause serious undesirable side effects, including cirrhosis, cholestatic jaundice, and elevated serum transaminase levels. Consequently, there is a need to explore gentler and lower cost treatments for nitrite toxicity and liver disease. Many herbal compounds contain polyphenols and flavonoids, which have anti-inflammatory and anti-oxidative effects. This has led to increased pharmacological interest in certain herbal medications. Thyme (*Thymus vulgaris*), an herb commonly used in cooking throughout the world, has antiseptic, antimicrobial, carminative, and anti-oxidative properties[15,16] and has been used to treat a range of human illnesses[17].

In traditional medicine, *T. vulgaris* has been used in a variety of ways because of its antiseptic, antispasmodic, anti-asthmatic, bronchodilator, expectorant, antitussive, carminative, anthelmintic, anti-microbial, and antioxidant qualities. It has been used to treat dyspepsia, chronic gastritis, diarrhea, and tonsillitis[18]. *T. vulgaris* extracts are believed to contain important anti-inflammatory and immunomodulator factors[19] with high free radical scavenging, anti-inflammatory, anti-platelet, anti-obesity, and anti-diabetic actions[17,20].

Monoterpenes and their hydrocarbons, as well as phenolics such as rosmarinic acid and flavonoid derivatives[21], are found in significant amounts in many species of thyme. The presence of these compounds renders thyme an important herb in research on antioxidants[22]. The aim of our study was to examine the protective effects of *T. vulgaris*, at both the cellular and biochemical levels, on $NaNO_2$-induced hepatic oxidative stress.

Materials and methods

Chemicals and kits. Kits for liver biomarkers, aspartate transaminase (AST), and alanine transaminase (ALT) were purchased from *Clini Lab* (Almanial; Cairo, Egypt). Kits for reduced glutathione (GSH), malondialdehyde (MDA), superoxide dismutase (SOD), and total proteins were purchased from Bio-diagnostic (Giza, Egypt). Chemicals used, including $NaNO_2$ and agarose, were purchased from Sigma-Aldrich (St. Louis, MO, USA). Kits for RNA reverse transcription were purchased from Fermentas (Thermo Fisher Scientific, Waltham, MA, USA). The QIAzol reagents were purchased from QIAGEN (Valencia, CA, USA).

Preparation of *T. vulgaris* extract. *T. vulgaris* leaves were collected from Taif markets in April 2020. Plants were identified by Dr. Yassin Alsodani a botanist at the College of Science, Taif University. The protocol and the methods used in this study was complied with relevant Taif University, Saudi Arabia and international guidelines and legislations. The extract was prepared according to the method used by Abdel-Aziem et al.[23]; the leaves were first air-dried, then powdered. The powder (100 g) was immersed in 500 mL ethanol (70%) and mixed. After 24 h, the mixture was filtered through Whatman paper No.1, then evaporated at 44 ± 1 °C in a vacuum. The solid extract (with a yield of 14.5% per 100 g of original material) was freeze-dried and stored at -20 C°.

Measurement of total polyphenolic and flavonoid compounds. Total polyphenols and flavonoids were estimated, with modifications, using a method previously described by Singleton et al.[24], who originally evaluated the total polyphenolic compounds in licorice extract using Foline-Ciocalteu reagent. This method has since been further developed and refined[25,26]. We combined 200 µL of sample (in triplicate) with 1 mL Folin-Ciocalteu reagent (10% v/v) and 800 µL 7.5% (w/v) Na_2CO_3, which was then incubated for 30 min at 25 °C. The optical density was measured spectrophotometrically at 760 nm, calibrated using a gallic acid standard curve. Values are presented in terms of mg gallic acid equivalent per 1 g dry thyme extract. Total flavonoid content was determined using an aluminum chloride colorimetric method[27], based on a rutin calibration curve (mg rutin equivalent per 1 g dry thyme extract).

Gas chromatography–mass spectrometry (GC–MS). GC–MS analysis was performed using a Focus GC model (Thermo Electron Corporation, Waltham, MA, USA) under specific conditions: (1) DB-5 capillary column (30 m × 0.32 mm, 0.50 mm); (2) column temperature 60 °C (1 min) to 180 °C at 3 °C/min; (3) injector and detector temperature 220 °C; (4) split ratio 1:10; (5) carrier gas He; flow rate: 1.0 mL/min. A sample aliquot of 1 µL was diluted in chloroform at a ratio of 1:10. GC retention indices and ratios were compared on polar columns with specific standard mass spectra[28].

Experimental design and animal handling. Twenty-eight mice (7 weeks old; 35 ± 2 g) were kept at 12 hr /12 hr light dark cycle in the animal quarters at Turabah University College, Taif University, Saudi Arabia. Mice were given free access to food and water and handled daily for 7 days to accustom them to human contact. The Ethical Committee of Turabah University College, Taif University approved all procedures and animal use for this study (project TURSP2020-09). Moreover, the study was carried out in compliance with the ARRIVE guidelines. The animals were split into four groups as follows: Group 1, the negative control group (CNT), received only saline orally; Group 2, the *T. vulgaris* control group, received 0.5 g/kg bw *T. vulgaris* extract orally for 15 days[23,29]; Group 3, the positive $NaNO_2$ intoxication group, received 60 mg/kg bw $NaNO_2$ orally on Day 14[30]; and Group 4, the protective group, received *T. vulgaris* extract as for Group 2, and then $NaNO_2$ on Day 14, as for Group 3. Figure 1 shows the details of the experimental protocol. We chose the dose of 60 mg/kg bw of $NaNO_2$ because, while this dose is not lethal, it will nevertheless cause significant toxicity, damaging tissues and cells, which can be measured clearly using biochemical assays[13,30,31].

On Day 15, 24 h after the final treatment, the mice were anesthetized and then euthanized by decapitation. Liver samples were taken and preserved in Qiazol for RNA extraction and qRT-PCR; histological samples were

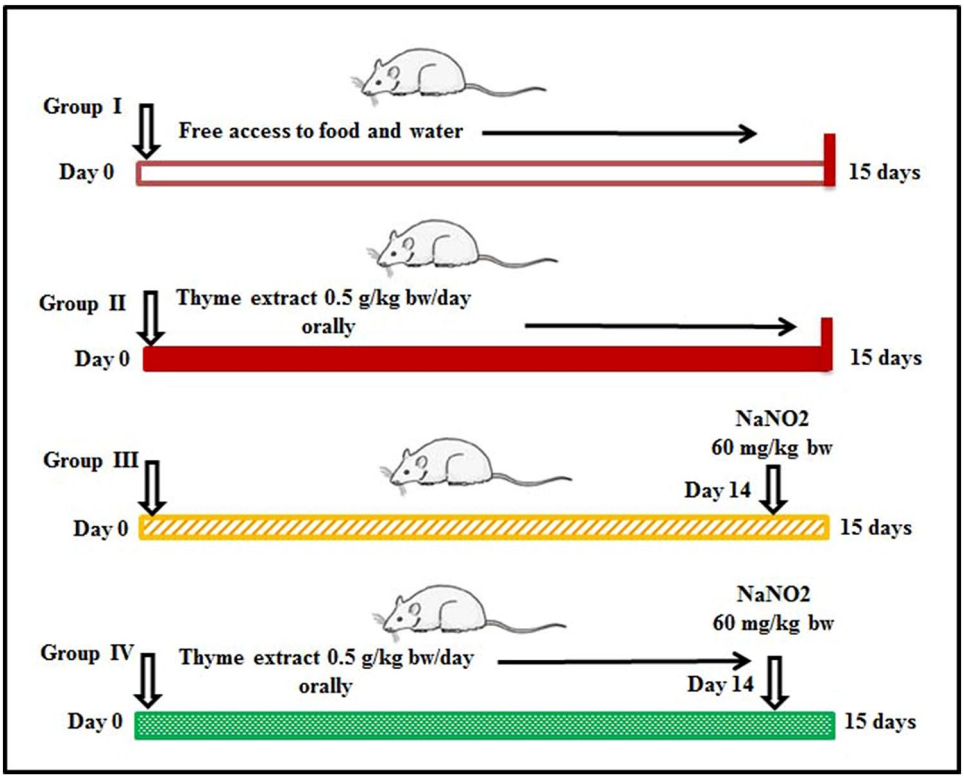

Figure 1. Schematic diagram showing the experimental design.

prepared using Bouin's solution; blood samples were collected and the extracted serum stored at -20 °C for later use.

Biochemical assessments. Serum ALT and AST levels were measured using a colorimetric spectrophotometer following the procedures in the user's manual. MDA levels were assessed using the technique developed by Ohkawa et al.[32]. SOD was measured using the method of Beutler et al.[33], reduced GSH using the method of Nishikimi et al.[34], and total protein levels were determined using the method of Lowry et al.[35]. These colorimetric methods were performed using a Bio-Rad Smart Tech Spectrophotometer according to the procedures in the product inserts provided with each kit. The reduced glutathione (GSH) and oxidized glutathione (GSSG) kits were purchased from Sigma-Aldrich Chemical (St. Louis, MO, USA). All chemicals used were of the highest purity and purchased from commercial suppliers in Saudi Arabia and Egypt.

Cytokine measurements. Several different kits for measuring parameters in mice, including mouse IL-1β (cat. No. E-EL-M0037), IL-6 (E-EL-M0044), and TNF-α (E-EL-M0049) were purchased from Elabscience (Houston, TX, USA). Serum cytokine levels were determined using Sandwich-ELISA kits in accordance with the product inserts and reference tables available at the Clinical Laboratory Sciences Department, Turabah University College, Taif University.

Quantitative real-time PCR (qRT-PCR) and gene expression. Total liver RNA was extracted and determined to be pure at 260/280 nm. Reverse transcription was performed using the Quanti-Tect reverse transcription kit with 1 µg total RNA, producing single-stranded complementary DNA (cDNA) using a two-step qRT-PCR reaction with a random primer hexamer. Amplification of cDNA was performed using SYBR Green master mix (Thermo Scientific, Waltham, MA, USA). Table 1 lists the primers used in thermal cycle qRT-PCR analysis, using the $2^{-\Delta\Delta Ct}$ method. β-actin was used as a 'house-keeping' (internal standard) gene, against which cDNA was normalized. Reactions were run on and analyzed using a 7500 FAST Real-Time PCR Detection System (Applied Biosystems, Foster City, CA, USA). qRT-PCR conditions were: 95 °C for 10 min (1st denaturation stage) and 40 cycles of 95 °C for 15 s (2nd denaturation stage) followed by 60 °C for 1 min (annealing and extension stage).

Changes in intensity and expression of the specific genes listed in Table 1 under Analysis were determined using comparative cycle threshold (CT) values.

Histological examinations. After decapitation, typical tissue specimens from the livers of all animals were harvested according to a standardized necropsy protocol[36] and immediately fixed in Bouin's solution for 24 h. The fixed specimens were thoroughly washed under running tap water, dehydrated in an ascending series

Gene	Accession number	Product size (bp)	Direction	Primer Sequence (5′–3′)
Thioredoxin	NM_011660.3	137 bp	Sense	5′-TGGAGAGGTGGCTCAGTCGT-3’
			Antisense	5′-GTGCCCATGGTGGCCAGTAG-3’
HO-1	NM_010442.2	126 bp	Sense	5′-CGCCTCCAGAGTTTCCGCAT-3’
			Antisense	5′-GACGCTCCATCACCGGACTG-3’
SOD	NM_011434.2	157 bp	Sense	5′-AGGACGGTGTGGCCAATGTG-3’
			Antisense	5′-CGGCTCCCAGCATTTCCAGT-3’
GSH synthase	NM_008180.2	139 bp	Sense	5′-CAGCCAGAACCCAGCCTTCC-3’
			Antisense	5′-GCGATTCAGGCCCAGGAACA
TNF-α	NM_013693.3	131 bp	Sense	5′-CACCATGAGCACAGAAAGCA-3’
			Antisense	5′-CTGCCACAAGCAGGAATGAG-3’
β-actin	NM_007393.5	140 bp	Sense	5′-CCAGCCTTCCTTCTTGGGTA-3’
			Antisense	5′-CAATGCCTGGGTACATGGTG-3’

Table 1. Primers used for quantitative real time PCR in mice.

of ethanol concentrations (70%, 80%, 90%, and 100%; 2 h each), cleared in two changes of xylene (1 h each), impregnated in two changes of soft paraffin (2 h each), embedded in paraffin blocks, cut into Sects. 4 µm thick, and routinely stained with hematoxylin and eosin following standard processing and staining protocols[37]. The stained sections were examined microscopically and any histopathological alterations observed were recorded. This was followed by multiparametric quantitative lesion scoring for the hepatic parenchyma in all groups following the protocol described by Khalil et al.[38] with a few modifications. For each animal, five randomly selected, non-duplicated microscopic profiles (40 × objective) were captured using an AmScope digital camera attached to an Olympus light microscope. These images were analyzed to allow calculation of the ratio of the area fractions of the hepatic central veins, portal blood vessels, sinusoids, necrosis, hemorrhage, fatty change, and leukocytic aggregations to the total areas using the image analysis software ImageJ (version 1.51v; Research Services Branch, NIH, Bethesda, MD, USA). The proportion of hepatic cells that exhibited pyknosis, single-cell necrosis, and vacuolar and hydropic degeneration with respect to the total number of hepatocytes per image was calculated subjectively. The frequency with which other lesions occurred (Kupffer cell hyperplasia, leukocytic infiltration, cholangiocyte hyperplasia and/or necrosis, and cholestasis) was determined by counting the number of lesions per image. Eventually, the results were expressed as percentages (mean ± SEM).

Statistical analysis. Seven mice per group were selected and one-way ANOVA and Dunnett's post hoc descriptive tests were performed using SPSS software version 22 (SPSS, IBM, Chicago, IL, USA) for Windows. The data are presented as mean ± standard error of mean; statistical significance is $p < 0.05$, indicated by letters with different symbols**.

Ethical Statement. All experimental procedures were carried out under National Institutes of Health Guidelines for the care and use of laboratory animals, and all procedures designed to minimize the suffering of animals were followed.

Results

Analysis and detection of *T. vulgaris* content. Analysis (using gallic acid as a standard curve) revealed that ethanolic *T. vulgaris* extract contained rosmarinic acid (38.23 mg/g dry weight thyme extract), luteolin-7-O-glucoside (17.3 mg/g), and caffeic acid (1.96 mg/g). These results are shown in Table 2. Concentrations of phenol and flavonoids were 221.65 and 115 mg/g, respectively, using rutin as a standard calibration curve (Table 1).

GC–MS analysis. Table 3 shows the major compounds contained in *T. vulgaris* extract. Ten major compounds were detected in *T. vulgaris* extract following GC–MS analysis; the molecular weight (MW), retention time (RT), and peak area vary among these compounds. The hydroxyl (OH), carbonyl (CO), acetyl ($COCH_3$), and nitro (NO_2) functional groups are also shown in Table 3.

Serum hepatic biomarkers. We observed elevated ALT and AST levels and lower total proteins in the $NaNO_2$-intoxicated groups (Groups 3 and 4), which indicated liver damage and dysfunction. In the group pretreated with *T.vulgaris* extract (Group 4), which received *T. vulgaris* extract for 14 days and then $NaNO_2$ for 24 h, we observed less pronounced changes in ALT and AST levels and total proteins (Table 4). Pretreatment with *T. vulgaris* extract normalized and returned ALT and AST levels and total proteins to their relative control levels.

Impact of *T. vulgaris* extract on oxidative stress biomarkers. Increased levels of MDA (a biomarker of lipid peroxidation), along with lower SOD serum levels, indicated tissue damage in the $NaNO_2$-intoxicated mice (Group 3). Group 2 mice, who received *T. vulgaris* only, exhibited moderate increases in SOD and GSH. In the $NaNO_2$-intoxicated mice (Group 4) pretreated with *T. vulgaris* extract, we observed alleviated GSH and SOD levels and a decrease in MDA levels, providing evidence for the ameliorative effect of the *T. vulgaris* extract

No	Name	Concentration
1	Caffeic acid	1.96 ± 0.53
2	Rosmarinic acid	38.23 ± 2.33
3	Luteolin	–
4	Luteolin-7-O-gluocoside	17.3 ± 1.034
5	Luteolin-7-O-rutinoside	–-
6	Apiginin	–
7	Apiginin–7-O-glucoside	–
8	Apiginin-7-O-rutinoside	–
9	Hesperdine	–
10	Hesperdine-7-O-glucoside	–
11	Hesperdine-7-O-rutinoside	–
12	Total Phenols	221.56 ± 6.8
13	Total flavonoids	115 ± 2

Table 2. Total Phenolic and flavonoids compounds identified in ethanolic extract of *Thymus vulgaris* for triplicate samples.

Item	RT (min)	Peak Area %	Class name	Molecular weight	Molecular Formula
1	9.7	2.51	Pyrrole derivative chelated with Nickel	715	$C_{44}H_{27}N_5NiO_2$
2	11.58	2.54	17-(5-ethyl-6-methylheptan-2-yl)-10,13-dimethyl-2,3,4,7,8,9,10,11,12,13,14,15,16,17-tetradec-ahydro-1H-cyclopenta[a]phenanthren-3-ol	414	$C_{29}H_{50}O$
3	11.69	2.44	3-((tert-butyldimethylsilyl)oxy)-13-methyl-7,8,9,11,12,13,14,15,16,17-decahydro-6H-cyclopenta[a]phenanthrene-16,17-diyl bis(2,2,3,3,3-pentafluoropropanoate)	694	$C_{30}H_{36}F_{10}O_5Si$
4	27.99	2.9	10-hydroxy-3a,6,6,9a,11a-pentamethyl-1-(6-methylheptan-2-yl)hexadecahydrocyclopenta[7,8] phenanthro[8a,9-b]oxiren-7-yl acetate	502	$C_{32}H_{54}O_4$
5	28.29	2.56	1-(2-hydroxy-7,9a,11b-trimethylhexadecahydrocyclopenta[1,2]phenanthro[8a,9-b]oxiren-9-yl) ethanone	346	$C_{22}H_{34}O_3$
6	32.39	2.97	8-methoxy-10a,12a-dimethyl-5-methylene-1-(6-methylheptan-2- yl)hexadecahydrocyclobuta[m] cyclopenta[a]phenanthren-6(4H)-one	454	$C_{31}H_{50}O_2$
7	41.69	2.44	N-(2-(2-acetyl-7-methoxy-1H-indol-3-yl)ethyl)benzenesulfonamide	372	$C_{19}H_{20}N_2O_4S$
8	44.62	2.69	dimethyl 3-(4-(5-hydroxy-1-(methoxycarbonyl)-1-methyldecahydronaphthalen-2-yl)butyl)-1-methoxy-7-methylnaphthalene-2,6-dicarboxylate	568	$C_{33}H_{44}O_8$
9	46.61	2.96	Ethyl 7-(4-hydroxy-3-methoxy-5-nitrophenyl)-5-methyl-4,7-dihydro-[1,2,4]triazolo[1,5-a] pyrimidine-6-carboxylate	375	$C_{16}H_{17}N_5O_6$
10	50.18	3.16	5,5′,8,8′-tetrahydroxy-6,6′-dimethyl-[2,2′-binaphthalene]-1,1′,4,4′-tetraone	406	$C_{22}H_{14}O_8$

Table 3. Compounds identified by Gas Chromatography-Mass Spectrometry (GC.MS) in ethanolic extract of *Thymus vulgaris*.

	ALT (U/l)	AST (U/l)	Total proteins (mg/dl)
Control	17.3 ± 0.6	24.9 ± 0.9	81.6 ± 6.9
Thyme Extract	23.5 ± 5.1	20.4 ± 1.8*	78.3 ± 2.5
$NaNO_2$	93.5 ± 4.3#	88.1 ± 3.3#	42.5 ± 4.5#
Thyme Extract + $NaNO_2$	44.5 ± 1.5$	41.6 ± 4.7$	66.5 ± 4.8$

Table 4. Protective effects of *Thymus vulgaris* extract against $NaNO_2$ induced alteration in liver biomarkers in mice. Values are means ± standard error (SEM) for 7 different mice per each treatment. Values are statistically significant at $^*p < 0.05$ versus control; $^\#p < 0.05$ versus control and thyme extract groups. $^\$p < 0.05$ versus $NaNO_2$. ALT: alanine transaminase; AST: aspartate transaminase.

against $NaNO_2$-induced hepatic toxicity (Table 5). The effect of *T. vulgaris* extract on the glutathione system was evaluated by determining the ratio of GSH to oxidized glutathione (GSSG) in serum from $NaNO_2$-intoxicated mice (Table 5). The *T. vulgaris* extract had a positive effect on the glutathione status in $NaNO_2$-injected mice by causing a concomitant increase in GSH levels and decrease in GSSG levels, which restored the GSH/GSSG ratio to control levels. The profound decrease in the GSH/GSSG ratio induced by $NaNO_2$ was normalized by *T. vulgaris* treatment for 15 days.

	MDA (nmol/ml)	SOD (U/ml)	GSH (nmol/l)	GSSG (nmol/l)	GSH/GSSGratio
Control	26.9 ± 0.89	3 ± 0.3	2.5 ± 0.6	1.1 ± 0.01	2.2 ± 0.02
Thyme Extract	28.3 ± 0.79	4.5 ± 0.7	3.3 ± 0.3	1.2 ± 0.01	2.73 ± 0.01
$NaNO_2$	69.2 ± 5.5$^{\#}$	1.6 ± 0.3$^{\#}$	1.1 ± 0.01$^{\#}$	0.79 ± 0.01$^{\#}$	1.25 ± 0.02$^{\#}$
Thyme Extract + $NaNO_2$	36.8 ± 1.4$^{\$}$	3.1 ± 0.6$^{\$}$	2.7 ± 0.2$^{\$}$	1.01 ± 0.02$^{\$}$	2.43 ± 0.07$^{\$}$

Table 5. Protective effects of *Thymus vulgaris* extract against $NaNO_2$ induced alterations in antioxidant activity in mice. Values are means ± SEM for 7 different mice per each experiment. Values are statistically significant at $^{\#}p < 0.05$ versus control and thyme extract groups. $^{\$}p < 0.05$ versus $NaNO_2$.

Measurements	Control	Thyme extract	$NaNO_2$	Thyme extract + $NaNO_2$
IL-1β (pg/ml)	156.7 ± 1.5	163 ± 24	308.2 ± 28$^{\#}$	165.7 ± 29.8$^{\$}$
IL-6 (pg/ml)	38.6 ± 1.4	43.7 ± 7	92.3 ± 3.8$^{\#}$	65.7 ± 13.3$^{\$}$
TNF-α (pg/ml)	235.3 ± 7.3	259 ± 19.3	427.3 ± 31.3$^{\#}$	273.7 ± 23$^{\$}$

Table 6. Protective effects of *Thymus vulgaris* extract against $NaNO_2$ induced changes in proinflammatory cytokines. Values are means ± SEM for 7 different mice per each experiment. Values are statistically significant at $^{\#}p < 0.05$ versus Control and Thyme Extract groups. $^{\$}p < 0.05$ versus $NaNO_2$. $NaNO_2$: Sodium nitrite.

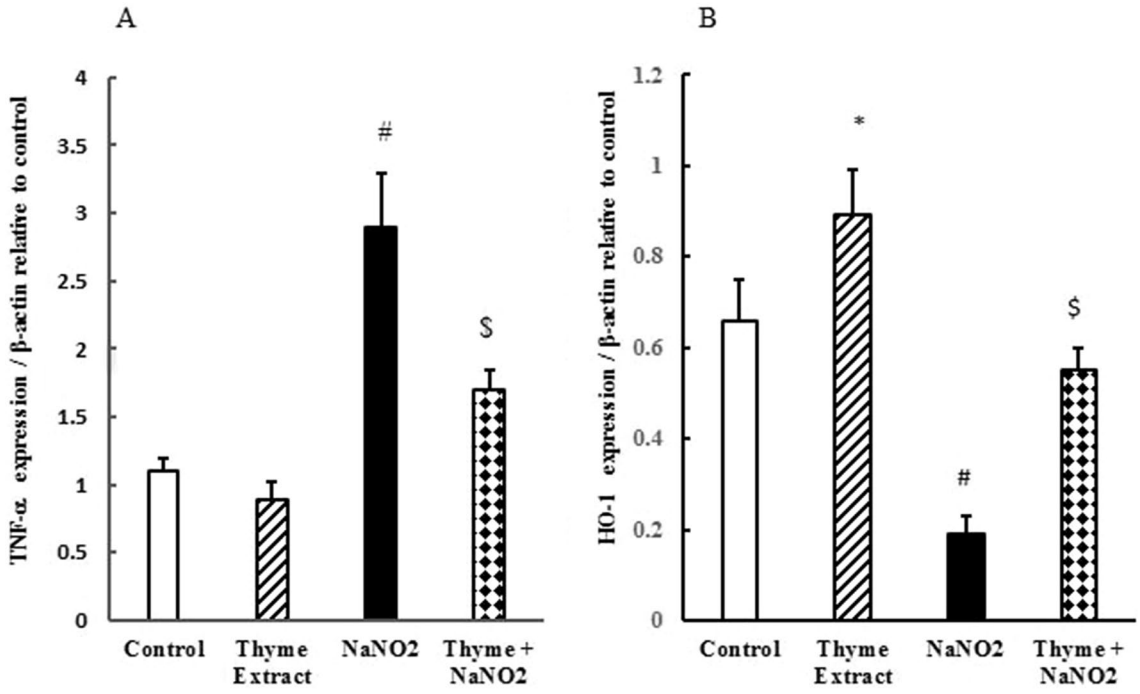

Figure 2. Ameliorative effect of *T. vulgaris* extract on mRNA expression of TNF-α (**A**) and HO-1 (**B**) in $NaNO_2$-treated mice. Graphic presentation of liver mRNA expression by qRT-PCR analysis of TNF-α (**A**) and HO-1 (**B**) in different groups of mice relative to β-actin. $^{*}p < 0.05$ versus the control group; $^{\#}p < 0.05$ versus the control and *T. vulgaris* extract groups; and $^{\$}p < 0.05$ versus the $NaNO_2$-treated group.

Mitigated impact of *T. vulgaris* extract on inflammatory cytokines. To examine the destructive impact of $NaNo_2$ on the immune state of mice, we measured the levels of pro-inflammatory cytokines. $NaNO_2$ injection increased serum levels of IL-1β, IL-6, and TNF-α in the $NaNO_2$-intoxicated mice (Groups 3 and 4). Pretreatment of $NaNO_2$-intoxicated mice with *T. vulgaris* (Group 4) mitigated these effects (Table 6), which eventually returned to normal levels. *T. vulgaris* extract normalized all altered pro-inflammatory cytokines.

Ameliorative effect of *T. vulgaris* extract on quantitative expression of liver genes. Nitrite toxicity induced liver damage and hepatic dysfunction as shown by the increases in hemeoxygenase-1 (HO-1), an oxidative stress biomarker, and TNF-α, an inflammatory cytokine (Fig. 2A,B). Gene expression for TNF-α

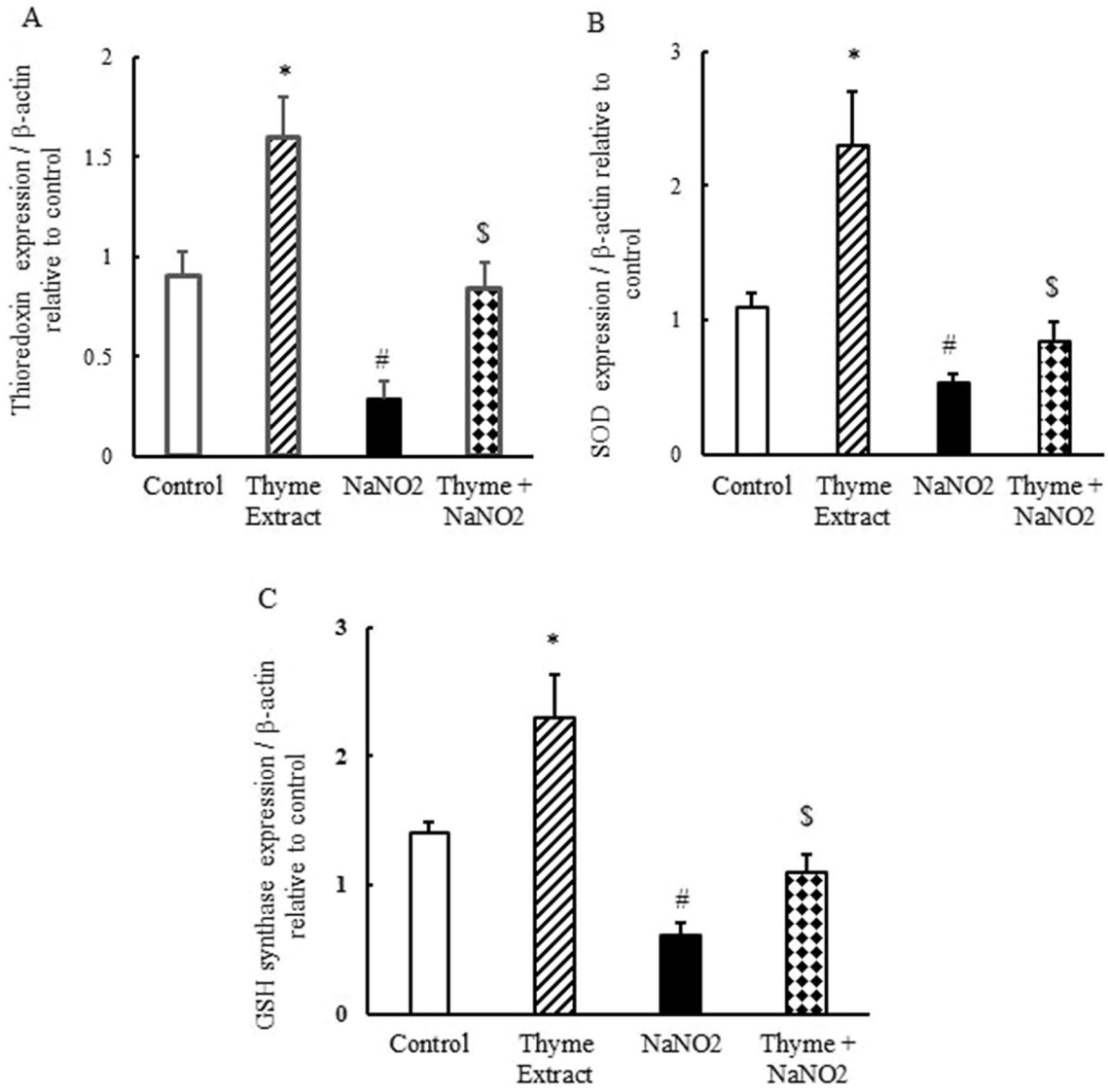

Figure 3. Ameliorative effect of *T. vulgaris* extract on mRNA expression of thioredoxin (**A**), SOD (**B**), and GSH synthase (**C**) in $NaNO_2$-treated mice. Graphic presentation of liver mRNA expression by qRT-PCR analysis of thioredoxin, SOD, and GSH synthase in different groups of mice relative to β-actin. $^{*}p < 0.05$ versus the control group; $^{\#}p < 0.05$ versus the control and *T. vulgaris* extract groups; and $^{\$}p < 0.05$ versus the $NaNO_2$-treated group.

mRNA was downregulated in the group pretreated with *T. vulgaris* extract (Fig. 2A). Conversely, the HO-1 gene was upregulated in the *T. vulgaris*-treated group (Fig. 2B). The ameliorative effects of *T. vulgaris* extract on both TNF-α and HO-1 expression and its potential to restore and recover gene alterations caused by $NaNO_2$ intoxication are shown in Fig. 2A,B.

Impact of *T. vulgaris* extract on quantitative expression of antioxidant genes in liver. qRT-PCR results showed that $NaNO_2$ downregulated thioredoxin, SOD, and GSH synthase mRNA expression (Fig. 3A–C), leading to oxidative stress in the liver. The *T.vulgaris*-treated group (Group 2) showed positive correlation in the antioxidant genes examined, as *T. vulgaris* upregulated thioredoxin, SOD, and GSH synthase mRNA expression, demonstrating that the extract has important antioxidative properties (Fig. 3). In the group pretreated with *T. vulgaris* extract for 14 days followed by $NaNO_2$ intoxication for 24 h (Group 4), the altered mRNA expression of the examined genes returned to within the normal range as a result of pretreatment.

Histopathological examination. Upon microscopic examination of the specimens taken from the control and *T. vulgaris*-treated animals, we observed normal hepatic histological architectures: roughly hexagon-shaped hepatic lobules with sinusoids converging from the periphery to the central vein and portal canals present at approximately three of the six angles of the lobule. The hepatic parenchyma between the portal canals consisted of hepatocytes arranged in cell plates (Fig. 4A,B). Exposure to $NaNO_2$ induced a wide variety of hepatopathic histological alterations, including circulatory changes (congestion of the central and portal veins and

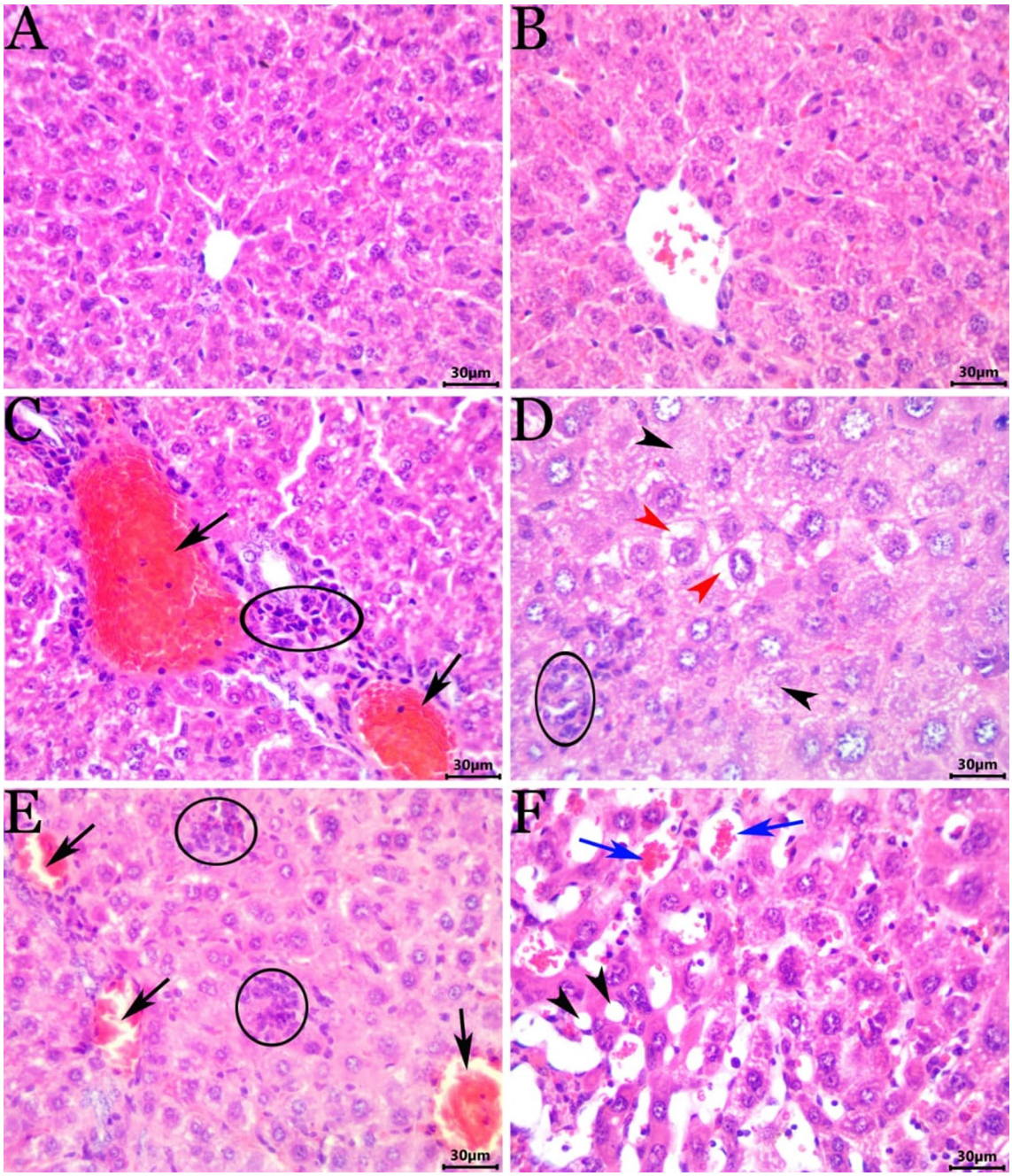

Figure 4. Representative photomicrograph of hematoxylin and eosin stained hepatic tissue sections showing the effects on the hepatic histology of exposure to $NaNO_2$ and/or *T. vulgaris*. (**A**) and (**B**), normal histological photomicrographs in the control and *T. vulgaris*-treated mice, respectively. (**C**) and (**D**), livers of the $NaNO_2$-treated mice showing portal congestion (arrows), inflammatory cell infiltrate (ellipses), cellular swelling associated with hydropic degeneration (red arrowheads), and single-cell necrosis (black arrowheads). (**E**) and (**F**), livers of $NaNO_2$ + *T. vulgaris*-treated mice showing focal mononuclear cell aggregates (ellipses), fatty change (black arrowheads), congested blood vessels (black arrows), and sinusoids (blue arrows).

sinusoids), hepatocyte degeneration and necrosis (pyknosis, cellular swelling associated with vacuolations due to vacuolar and hydropic degenerations or fatty changes, and single cell necrosis), and inflammatory changes (intralobular and/or leukocytic infiltration or aggregations) (Fig. 4C,D). Interestingly, the biliary system did not show any noticeable histological alterations. *T. vulgaris* showed marked hepatoprotective effects against the $NaNO_2$-induced hepatopathy. Although the hepatic tissue sections from the $NaNO_2$ + *T. vulgaris*-treated animals were not completely histologically normal, we observed a significant reduction in the severity and frequency of the $NaNO_2$-induced histological changes. The most frequent lesions in this group were vacuolar vascular congestion, sinusoidal dilatation, hepatocyte vacuolation, and tiny mononuclear cell aggregations (Fig. 4E,F).

Lesion	Control	Thymus extract	$NaNO_2$	GA3 + $NaNO_2$
Central vein	2.2 ± 0.4^a	2.17 ± 0.03^a	2.7 ± 0.1^a	2.4 ± 0.06^a
Portal blood vessels	1.4 ± 0.06^a	$1.33 \pm .0\ 07^a$	3.9 ± 0.13^b	2.2 ± 0.09^c
Sinusoidal spaces	6.3 ± 0.12^a	6.7 ± 0.1^a	9.01 ± 0.2^b	8.0 ± 0.1^c
fatty change	0^a	0^a	0.6 ± 0.1^b	0.18 ± 0.09^c
Focal leukocytic aggregation	0^a	0^a	0.77 ± 0.02^b	0.29 ± 0.1^c
Focal necrosis	0^a	0^a	0.1 ± 0.07^b	0.04 ± 0.01^c
Vacuolar and hydropic degeneration	0^a	0^a	26.2 ± 4.8^b	17.5 ± 4.6^c
Hepatocyte pyknosis	0^a	0^a	2.1 ± 0.4^b	0.6 ± 0.2^c
single-cell Necrosis	0^a	0^a	1.6 ± 0.4^b	0.4 ± 0.1^c
Cholestasis	0^a	0^a	0.0^a	$0.\ 17 \pm 0.002^c$
cholangeocyte hyperplasia	0^a	0^a	0^a	0^a
Von Kupffer cellhyperplasia	0^a	0^a	4.6 ± 0.2^b	3.2 ± 0.3^c
Inflammatory infiltrate	0^a	0^a	23 ± 0.5^b	9.1 ± 2.9^c

Table 7. Analysis and lesion scoring in the hepatic tissues of mice in response to $NaNO_2$ and *thymus vulgaris* treatment. Values are expressed as means ± SEM for 7 different mice per each treatment. Values with different letters means signficant at $p < 0.05$ beteweengroups.

The overall hepatic lesion scoring changes induced by $NaNO_2$ and possible amelioration by thymus extract are shown in Table 7.

Discussion

Our study confirmed that $NaNO_2$ intoxication increases the levels of ALT and AST in serum, decreases total proteins, affects cytokine levels and gene expression (leading to an imbalance in antioxidant mechanisms), and causes histopathological changes, resulting in severe oxidative stress in liver tissues. However, pretreatment with *T. vulgaris* extract prevented or reversed these effects, confirming the antioxidant effect of *T. vulgaris* against $NaNO_2$-induced hepatic dysfunction.

The elevated levels of ALT and AST, decreased total serum proteins, and the histopathological alterations that we observed, are all indicators of toxicity and also well-known quantitative measures of liver activity[39]. While functional liver damage can be indicated by high serum levels of AST, a more liver-specific indicator is the enzyme ALT. ALT catalyzes the conversion of alanine into pyruvate and glutamate, making serum levels of ALT a more reliable indicator of liver damage[40]. Our findings demonstrated that the membrane structure and integrity of the liver cells, which would otherwise have been destroyed by $NaNO_2$, remained undamaged and uncongested, providing strong evidence for the protective effect of *T. vulgaris* extract also described previously[17,41].

Sharma et al.[42] noted that hepatoprotective plants are characterized by significant levels of polyphenols and flavonoids, major compounds also found in *T. vulgaris*. Flavonoids promote the expression of enzymes involved in the production of glutamylcysteine synthetase and thioredoxin, leading to increased intracellular GSH levels[43,44]. The antioxidant assays used in this study, which targeted five different types of ROS molecules (MDA, SOD, GSH, GSSG, and GSH/GSSG), confirmed the strong antioxidant effect of the *T. vulgaris* extract. Our findings are in agreement with those of previous studies that reported the high phenolic content and strong antioxidative effect of *T. vulgaris* extract[17]. Inhibition and decreased function of the antioxidant system causes the accumulation of H_2O_2 and hepatic cell decomposition[45]. Treatment with *T. vulgaris* extract significantly reversed these decreases in antioxidant enzyme activity.

Our study showed that $NaNO_2$ intoxication reduced antioxidant activity and increased both oxidative stress and lipid peroxidation in agreement with previous reports[11,30]. Antioxidant defenses are affected by the expression of genes such as thioredoxin, SOD, and GSH[46], and oxidative stress is regulated by several other downstream genes, including HO-1[47]. Hyun[48] showed that many plant extracts play a critical role in increasing antioxidant activity and reducing ROS. Overexpression of a particular hemoxygenase-1 reported here in thymus control group and downregulation in the $NaNO_2$-treated groups, confirmed the potential of *T. vulgaris* extract. HO-1 is normally involved in the regulation of mitochondrial biogenesis, neurogenesis, and angiogenesis[48], causing an increase in protein expression[49]. As such, HO-1 plays an important role in mechanisms of oxidative stress and inflammation[50]. By controlling IL-1β activation[51], HO-1 regulated the expression of inflammasome-associated genes[52]. The antioxidant mechanism is regulated by downstream genes that control oxidative stress, such as Nrf2 and HO-1[47,53]. Our findings confirmed that HO-1 expression plays a key role in the regulation of hepatic oxidative stress regulated by *T. vulgaris* extract. To explore the potential mechanism underlying the hepatoprotective effect of *T. vulgaris* extract, we examined the role of HO-1 signaling. Most reports have indicated that HO-1 plays a role in the activation and expression of some antioxidant and anti-inflammatory cytokine genes[54,55]. All were coincided with our reported findings.

Our study confirmed that *T. vulgaris* extract regulated the expression of pro-inflammatory cytokines, such as IL-1β, thereby ameliorating the $NaNO_2$-induced inflammatory response. The inflammatory response causes increased production of IL-1β, IL-6, and TNF-α cytokines[56], which play a leading role in sepsis and fever. $NaNO_2$ intoxication has the same effect[57], yet our study found that cytokine levels in mice pretreated with *T. vulgaris*

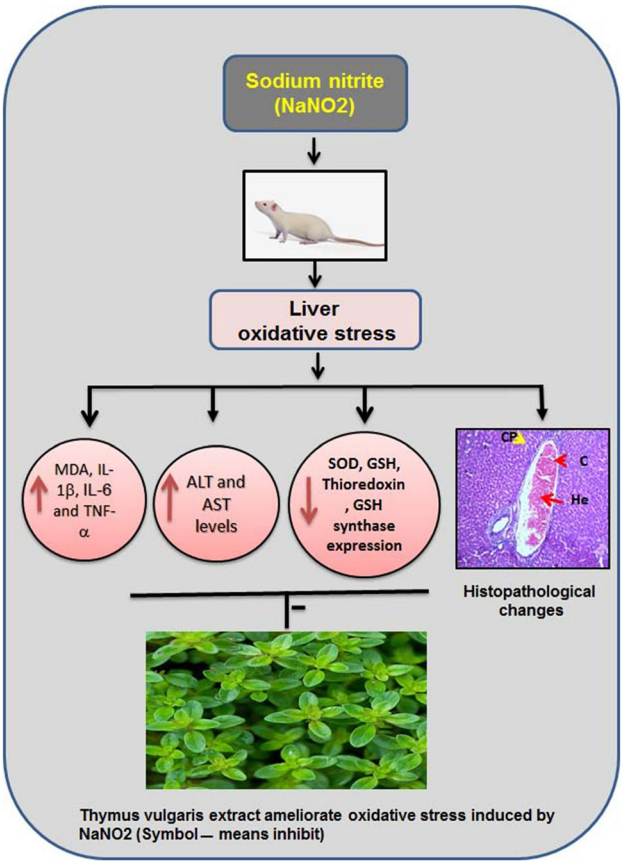

Figure 5. Schematic representation of the ameliorative effect of *T. vulgaris* extract on liver dysfunction. $NaNO_2$ intoxication induced hepatic dysfunction, decreased antioxidant activity, and an increase in the levels and expression of inflammatory cytokines. These results of treatment with $NaNO_2$ were normalized by pretreatment with *T. vulgaris* extract.

extract returned to normal. Therefore, *T. vulgaris* extract prevented $NaNO_2$-induced hepatic toxicity by ameliorating disrupted serum levels of IL-1β, IL-6, and TNF-α.

Reactive oxygen species (ROS) play a vital role in maintaining various human physiological processes[58], but at high levels, they can be cytotoxic and cause liver damage[59]. Therefore, mechanisms exist to maintain appropriate ROS levels in the liver and other organs, thereby preventing oxidative stress and promoting redox homeostasis[59]. Our study found that while $NaNO_2$ intoxication induced lipid peroxidation, pretreatment with *T. vulgaris* reversed these effects. In part, this was due to the recovery of depleted GSH, which plays a significant defensive role against oxidative stress[60].

Hydroperoxides are converted into alcohols and water in a process catalyzed by thioredoxin, a cytosolic protein[61]. Thioredoxin has several antioxidant functions, including scavenging for free radicals, removing hydrogen peroxide, protecting against oxidative stress, as well as broader functions in genetic transcription, DNA and protein repair, immunostimulant roles, apoptosis, and cell proliferation. As a thiol-specific antioxidant, thioredoxin shares many of the same functions as glutathione systems and the two are understood to act in tandem in the management of oxidative stress[62]. In our study, $NaNO_2$ downregulated thioredoxin and GSH synthase expression, but these returned to normal in mice pretreated with *T. vulgaris* extract.

In addition to biochemical alterations, the hepatotoxic effect of $NaNO_2$ has been further implicated in a wide variety of degenerative, circulatory, and inflammatory alterations. The etiopathogenesis of these hepatopathic morphological alterations are likely to be multifactorial and mediated by $NaNO_2$-induced oxidative damage and inflammation due to the formation of ROS and lipid peroxidation. The latter is associated with lysosomal and mitochondrial membrane rupture and subsequent release of digestive proteases[63] and activation of the apoptosis-related Bax and caspase-3 genes[64].

Treatment with $NaNO_2$ caused hepatic dysfunction, oxidative stress, and alteration in the levels of inflammatory cytokines. Pretreatment with *T. vulgaris* extract alleviated these responses to toxicity and restored the levels and mRNA expression of the proteins and genes. The collective summary for the protective impact of *T. vulgaris* on $NaNO_2$-induced liver dysfunction are clearly shown in Fig. 5.

Conclusion

T. vulgaris extract exerted a protective effect against oxidative stress in liver tissues caused by $NaNO_2$ intoxication. The effect was observed in different antioxidant systems and through the regulation of pro-inflammatory cytokines. In short, the common herb thyme (*T. vulgaris*) can be used in the prevention and treatment of hepatic oxidative stress.

Data availability

Data are available upon request.

Received: 24 October 2020; Accepted: 28 February 2021
Published online: 11 March 2021

References

1. Carlström, M. *et al.* Dietary nitrate attenuates oxidative stress, prevents cardiac and renal injuries, and reduces blood pressure in salt-induced hypertension. *Cardiovasc. Res.* **89**, 574–585. https://doi.org/10.1093/cvr/cvq366 (2011).
2. McNally, B., Griffin, J. L. & Roberts, L. D. Dietary inorganic nitrate: from villain to hero in metabolic disease?. *Mol. Nutr. Food Res.* **60**, 67–78. https://doi.org/10.1002/mnfr.201500153 (2016).
3. Lundberg, J. O., Weitzberg, E. & Gladwin, M. T. The nitrate-nitrite-nitric oxide pathway in physiology and therapeutics. *Nat. Rev. Drug Discov.* **7**, 156–167. https://doi.org/10.1038/nrd2466 (2008).
4. Shiva, S. Nitrite: a physiological store of nitric oxide and modulator of mitochondrial function. *Redox Biol.* **1**, 40–44. https://doi.org/10.1016/j.redox.2012.11.005 (2013).
5. Butler, A. R. & Feelisch, M. Therapeutic uses of inorganic nitrite and nitrate: from the past to the future. *Circulation* **117**, 2151–2159. https://doi.org/10.1161/circulationaha.107.753814 (2008).
6. Nossaman, V. E., Nossaman, B. D. & Kadowitz, P. J. Nitrates and nitrites in the treatment of ischemic cardiac disease. *Cardiol. Rev.* **18**, 190–197. https://doi.org/10.1097/CRD.0b013e3181c8e14a (2010).
7. King, A. M., Glass, K. A., Milkowski, A. L. & Sindelar, J. J. Impact of clean-label antimicrobials and nitrite derived from natural sources on the outgrowth of clostridium perfringens during cooling of deli-style Turkey breast. *J. Food Prot.* **78**, 946–953. https://doi.org/10.4315/0362-028x.Jfp-14-503 (2015).
8. Al-Rasheed, N. M., Fadda, L. M., Attia, H. A., Ali, H. M. & Al-Rasheed, N. M. Quercetin inhibits sodium nitrite-induced inflammation and apoptosis in different rats organs by suppressing Bax, HIF1-α, TGF-β, Smad-2, and AKT pathways. *J. Biochem. Mol. Toxicol.* https://doi.org/10.1002/jbt.21883 (2017).
9. Chui, J. S., Poon, W. T., Chan, K. C., Chan, A. Y. & Buckley, T. A. Nitrite-induced methaemoglobinaemia—aetiology, diagnosis and treatment. *Anaesthesia* **60**, 496–500. https://doi.org/10.1111/j.1365-2044.2004.04076.x (2005).
10. Ansari, F. A., Ali, S. N., Arif, H., Khan, A. A. & Mahmood, R. Acute oral dose of sodium nitrite induces redox imbalance, DNA damage, metabolic and histological changes in rat intestine. *PLoS ONE* **12**, e0175196. https://doi.org/10.1371/journal.pone.0175196 (2017).
11. Ansari, F. A. & Mahmood, R. Sodium nitrite enhances generation of reactive oxygen species that decrease antioxidant power and inhibit plasma membrane redox system of human erythrocytes. *Cell Biol. Int.* **40**, 887–894. https://doi.org/10.1002/cbin.10628 (2016).
12. Sherif, I. O. & Al-Gayyar, M. M. Antioxidant, anti-inflammatory and hepatoprotective effects of silymarin on hepatic dysfunction induced by sodium nitrite. *Eur. Cytokine Netw.* **24**, 114–121. https://doi.org/10.1684/ecn.2013.0341 (2013).
13. Ansari, F. A., Ali, S. N., Khan, A. A. & Mahmood, R. Acute oral dose of sodium nitrite causes redox imbalance and DNA damage in rat kidney. *J. Cell. Biochem.* **119**, 3744–3754. https://doi.org/10.1002/jcb.26611 (2018).
14. Eissa, M. M. *et al.* Chlorella vulgaris ameliorates sodium nitrite-induced hepatotoxicity in rats. *Environ. Sci. Pollut. Res. Int.* https://doi.org/10.1007/s11356-020-11474-9 (2020).
15. Ulukanli, Z., Cigremis, Y. & Ilcim, A. In vitro antimicrobial and antioxidant activity of acetone and methanol extracts from Thymus leucotrichius (Lamiaceae). *Eur. Rev. Med. Pharmacol. Sci.* **15**, 649–657 (2011).
16. Sajed, H., Sahebkar, A. & Iranshahi, M. *Zataria multiflora* Boiss. (Shirazi thyme)—an ancient condiment with modern pharmaceutical uses. *J. Ethnopharmacol.* **145**, 686–698. https://doi.org/10.1016/j.jep.2012.12.018 (2013).
17. El-Nekeety, A. A. *et al.* Antioxidant properties of *Thymus vulgaris* oil against aflatoxin-induce oxidative stress in male rats. *Toxicon* **57**, 984–991. https://doi.org/10.1016/j.toxicon.2011.03.021 (2011).
18. Pina-Vaz, C. *et al.* Antifungal activity of *Thymus oils* and their major compounds. *J. Eur. Acad. Dermatol. Venereol. JEADV* **18**, 73–78. https://doi.org/10.1111/j.1468-3083.2004.00886.x (2004).
19. Ocaña, A. & Reglero, G. Effects of thyme extract oils (from *Thymus vulgaris*, *Thymus zygis*, and *Thymus hyemalis*) on cytokine production and gene expression of oxLDL-stimulated THP-1-macrophages. *J. Obes.* **2012**, 104706. https://doi.org/10.1155/2012/104706 (2012).
20. Vigo, E., Cepeda, A., Gualillo, O. & Perez-Fernandez, R. In-vitro anti-inflammatory effect of *Eucalyptus globulus* and *Thymus vulgaris*: nitric oxide inhibition in J774A.1 murine macrophages. *J. Pharm. Pharmacol.* **56**, 257–263. https://doi.org/10.1211/0022357022665 (2004).
21. Schött, G. *et al.* The chemical composition of the pharmacologically active Thymus species, its antibacterial activity against Streptococcus mutans and the antiadherent effects of *T. vulgaris* on the bacterial colonization of the in situ pellicle. *Fitoterapia* **121**, 118–128. https://doi.org/10.1016/j.fitote.2017.07.005 (2017).
22. El-Boshy, M. E. *et al.* The remedial effect of *Thymus vulgaris* extract against lead toxicity-induced oxidative stress, hepatorenal damage, immunosuppression, and hematological disorders in rats. *Environ. Sci. Pollut. Res. Int.* **26**, 22736–22746. https://doi.org/10.1007/s11356-019-05562-8 (2019).
23. Abdel-Aziem, S. H. *et al.* Ameliorative effects of thyme and calendula extracts alone or in combination against aflatoxins-induced oxidative stress and genotoxicity in rat liver. *Cytotechnology* **66**, 457–470. https://doi.org/10.1007/s10616-013-9598-7 (2014).
24. Singleton, V. L., Orthofer, R. & Lamuela-Raventós, R. M. *Methods in Enzymology* Vol. 299, 152–178 (Elsevier, Amsterdam, 1999).
25. Ordonez, A., Gomez, J. & Vattuone, M. Antioxidant activities of *Sechium edule* (Jacq.) Swartz extracts. *Food Chem.* **97**, 452–458 (2006).
26. Naczk, M. & Shahidi, F. Phenolics in cereals, fruits and vegetables: occurrence, extraction and analysis. *J. Pharm. Biomed. Anal.* **41**, 1523–1542. https://doi.org/10.1016/j.jpba.2006.04.002 (2006).
27. Rezzoug, M. *et al.* Chemical composition and bioactivity of essential oils and Ethanolic extracts of *Ocimum basilicum* L. and *Thymus algeriensis* Boiss. & Reut. from the Algerian Saharan Atlas. *BMC Complement. Altern. Med.* **19**, 146. https://doi.org/10.1186/s12906-019-2556-y (2019).
28. Heidari, Z., Salehzadeh, A., Sadat Shandiz, S. A. & Tajdoost, S. Anti-cancer and anti-oxidant properties of ethanolic leaf extract of Thymus vulgaris and its bio-functionalized silver nanoparticles. *3 Biotech* **8**, 177. https://doi.org/10.1007/s13205-018-1199-x (2018).

29. Abdel-Azeem, A. S., Hegazy, A. M., Zeidan, H. M., Ibrahim, K. S. & El-Sayed, E. M. Potential renoprotective effects of rosemary and thyme against gentamicin toxicity in rats. *J. Diet. Suppl.* **14**, 380–394. https://doi.org/10.1080/19390211.2016.1253632 (2017).
30. Ansari, F. A., Khan, A. A. & Mahmood, R. Protective effect of carnosine and N-acetylcysteine against sodium nitrite-induced oxidative stress and DNA damage in rat intestine. *Environ. Sci. Pollut. Res. Int.* **25**, 19380–19392. https://doi.org/10.1007/s11356-018-2133-9 (2018).
31. Ansari, F. A., Khan, A. A. & Mahmood, R. Ameliorative effect of carnosine and N-acetylcysteine against sodium nitrite induced nephrotoxicity in rats. *J. Cell. Biochem.* https://doi.org/10.1002/jcb.27971 (2018).
32. Ohkawa, H., Ohishi, N. & Yagi, K. Assay for lipid peroxides in animal tissues by thiobarbituric acid reaction. *Anal. Biochem.* **95**, 351–358. https://doi.org/10.1016/0003-2697(79)90738-3 (1979).
33. Beutler, E., Duron, O. & Kelly, B. M. Improved method for the determination of blood glutathione. *J. Lab. Clin. Med.* **61**, 882–888 (1963).
34. Nishikimi, M., Appaji, N. & Yagi, K. The occurrence of superoxide anion in the reaction of reduced phenazine methosulfate and molecular oxygen. *Biochem. Biophys. Res. Commun.* **46**, 849–854. https://doi.org/10.1016/s0006-291x(72)80218-3 (1972).
35. Lowry, O. H., Rosebrough, N. J., Farr, A. L. & Randall, R. J. Protein measurement with the Folin phenol reagent. *J. Biol. Chem.* **193**, 265–275 (1951).
36. Ruehl-Fehlert, C. *et al.* Revised guides for organ sampling and trimming in rats and mice–part 1. *Exp. Toxicol. Pathol.* **55**, 91–106 (2003).
37. Slaoui, M. & Fiette, L. Histopathology procedures: from tissue sampling to histopathological evaluation. *Methods Mol. Biol. (Clifton, N.J.)* **691**, 69–82. https://doi.org/10.1007/978-1-60761-849-2_4 (2011).
38. Khalil, S. R. *et al.* Protective effect of Spirulina platensis against physiological, ultrastructural and cell proliferation damage induced by furan in kidney and liver of rat. *Ecotoxicol. Environ. Saf.* **192**, 110256. https://doi.org/10.1016/j.ecoenv.2020.110256 (2020).
39. Grespan, R. *et al.* Hepatoprotective effect of pretreatment with *Thymus vulgaris* essential oil in experimental model of acetaminophen-induced injury. *Evid. Based Complement. Altern. Med. eCAM* **2014**, 954136. https://doi.org/10.1155/2014/954136 (2014).
40. Sallie, R., Tredger, J. M. & Williams, R. Drugs and the liver. Part 1: testing liver function. *Biopharm. Drug Dispos.* **12**, 251–259. https://doi.org/10.1002/bdd.2510120403 (1991).
41. Zhang, X. *et al.* Ameliorative effect of supercritical fluid extract of Chrysanthemum indicum Linnén against D-galactose induced brain and liver injury in senescent mice via suppression of oxidative stress, inflammation and apoptosis. *J. Ethnopharmacol.* **234**, 44–56. https://doi.org/10.1016/j.jep.2018.12.050 (2019).
42. Sharma, A., Sangameswaran, B., Jain, V. & Saluja, M. J. I. C. P. J. Hepatoprotective activity of *Adina cordifolia* against ethanol induce hepatotoxicity in rats. *Int. Curr. Pharm. J.* **1**, 279–284 (2012).
43. Myhrstad, M. C., Carlsen, H., Nordström, O., Blomhoff, R. & Moskaug, J. Flavonoids increase the intracellular glutathione level by transactivation of the gamma-glutamylcysteine synthetase catalytical subunit promoter. *Free Radical Biol. Med.* **32**, 386–393. https://doi.org/10.1016/s0891-5849(01)00812-7 (2002).
44. Moskaug, J., Carlsen, H., Myhrstad, M. C. & Blomhoff, R. Polyphenols and glutathione synthesis regulation. *Am. J. Clin. Nutr.* **81**, 277s–283s. https://doi.org/10.1093/ajcn/81.1.277S (2005).
45. Halliwell, B. Free radicals, antioxidants, and human disease: curiosity, cause, or consequence?. *Lancet (London, England)* **344**, 721–724. https://doi.org/10.1016/s0140-6736(94)92211-x (1994).
46. Khafaga, A. F. & El-Sayed, Y. S. Spirulina ameliorates methotrexate hepatotoxicity via antioxidant, immune stimulation, and pro-inflammatory cytokines and apoptotic proteins modulation. *Life Sci.* **196**, 9–17. https://doi.org/10.1016/j.lfs.2018.01.010 (2018).
47. Ge, M. *et al.* Brg1-mediated Nrf2/HO-1 pathway activation alleviates hepatic ischemia-reperfusion injury. *Cell Death Dis.* **8**, e2841. https://doi.org/10.1038/cddis.2017.236 (2017).
48. Hyun, T. K., Kim, H.-C. & Kim, J.-S. Antioxidant and antidiabetic activity of Thymus quinquecostatus Celak. *Ind. Crops Prod.* **52**, 611–616 (2014).
49. Hull, T. D. *et al.* Heme oxygenase-1 regulates mitochondrial quality control in the heart. *JCI Insight* **1**, e85817. https://doi.org/10.1172/jci.insight.85817 (2016).
50. Abdou, K. H., Moselhy, W. A., Mohamed, H. M., El-Nahass, E. S. & Khalifa, A. G. Moringa oleifera leaves extract protects titanium dioxide nanoparticles-induced nephrotoxicity via Nrf2/HO-1 signaling and amelioration of oxidative stress. *Biol. Trace Elem. Res.* **187**, 181–191. https://doi.org/10.1007/s12011-018-1366-2 (2019).
51. Abd El-Twab, S. M., Hussein, O. E., Hozayen, W. G., Bin-Jumah, M. & Mahmoud, A. M. Chicoric acid prevents methotrexate-induced kidney injury by suppressing NF-kappaB/NLRP3 inflammasome activation and up-regulating Nrf2/ARE/HO-1 signaling. *Inflamm. Res.* **68**, 511–523. https://doi.org/10.1007/s00011-019-01241-z (2019).
52. Szabo, G. & Csak, T. Inflammasomes in liver diseases. *J. Hepatol.* **57**, 642–654. https://doi.org/10.1016/j.jhep.2012.03.035 (2012).
53. Li, J. *et al.* Xiaochaihutang attenuates liver fibrosis by activation of Nrf2 pathway in rats. *Biomed. Pharmacother.* **96**, 847–853. https://doi.org/10.1016/j.biopha.2017.10.065 (2017).
54. Abd El-Twab, S. M., Hozayen, W. G., Hussein, O. E. & Mahmoud, A. M. 18β-Glycyrrhetinic acid protects against methotrexate-induced kidney injury by up-regulating the Nrf2/ARE/HO-1 pathway and endogenous antioxidants. *Renal Fail.* **38**, 1516–1527. https://doi.org/10.1080/0886022x.2016.1216722 (2016).
55. Mahmoud, A. M., Hozayen, W. G. & Ramadan, S. M. Berberine ameliorates methotrexate-induced liver injury by activating Nrf2/HO-1 pathway and PPARγ, and suppressing oxidative stress and apoptosis in rats. *Biomed. Pharmacother.* **94**, 280–291. https://doi.org/10.1016/j.biopha.2017.07.101 (2017).
56. Bhatia, M. & Moochhala, S. Role of inflammatory mediators in the pathophysiology of acute respiratory distress syndrome. *J. Pathol.* **202**, 145–156. https://doi.org/10.1002/path.1491 (2004).
57. Sherif, I. O. & Al-Gayyar, M. M. Cod liver oil in sodium nitrite induced hepatic injury: does it have a potential protective effect?. *Redox Rep. Commun. Free Radical Res.* **20**, 11–16. https://doi.org/10.1179/1351000214y.0000000097 (2015).
58. Finkel, T. Signal transduction by reactive oxygen species. *J. Cell Biol.* **194**, 7–15. https://doi.org/10.1083/jcb.201102095 (2011).
59. Willcox, J. K., Ash, S. L. & Catignani, G. L. Antioxidants and prevention of chronic disease. *Crit. Rev. Food Sci. Nutr.* **44**, 275–295. https://doi.org/10.1080/10408690490468489 (2004).
60. Gutiérrez, M. B., Miguel, B. S., Villares, C., Gallego, J. G. & Tuñón, M. J. Oxidative stress induced by Cremophor EL is not accompanied by changes in NF-kappaB activation or iNOS expression. *Toxicology* **222**, 125–131. https://doi.org/10.1016/j.tox.2006.02.002 (2006).
61. Lu, J. & Holmgren, A. The thioredoxin antioxidant system. *Free Radical Biol. Med.* **66**, 75–87. https://doi.org/10.1016/j.freeradbiomed.2013.07.036 (2014).
62. Telorack, M. *et al.* A glutathione-Nrf2-thioredoxin cross-talk ensures keratinocyte survival and efficient wound repair. *PLoS Genet.* **12**, e1005800. https://doi.org/10.1371/journal.pgen.1005800 (2016).
63. Kiani, A., Yousefsani, B. S., Doroudian, P., Seydi, E. & Pourahmad, J. The mechanism of hepatotoxic effects of sodium nitrite on isolated rat hepatocytes. *Toxicol. Environ. Health Sci.* **9**, 244–250. https://doi.org/10.1007/s13530-017-0327-z (2017).
64. El-Nabarawy, N. A., Gouda, A. S., Khattab, M. A. & Rashed, L. A. Effects of nitrite graded doses on hepatotoxicity and nephrotoxicity, histopathological alterations, and activation of apoptosis in adult rats. *Environ. Sci. Pollut. Res. Int.* **27**, 14019–14032. https://doi.org/10.1007/s11356-020-07901-6 (2020).

Acknowledgements
We appreciate and thank Taif University for the financial support for Taif University Researchers Supporting Project (TURSP-2020/09), Taif University, Taif, Saudi Arabia.

Author contributions
M.M.S.: designed, supervise experiments, analyzed data and wrote the paper. A.A.: Analyzed data, Real time PCR, Chemistry analysis. M.M.M.M.: Histopathology and Revised paper.

Funding
This study was supported by Taif University Researchers Supporting Project (TURSP-2020/09), Taif University, Taif, Saudi Arabia.

Competing interests
The authors declare no competing interests.

Additional information
Correspondence and requests for materials should be addressed to M.M.S.

Reprints and permissions information is available at www.nature.com/reprints.

Publisher's note Springer Nature remains neutral with regard to jurisdictional claims in published maps and institutional affiliations.